SARS-CoV-2 and HSV-1 Induce Amyloid Aggregation in Human CSF

Wanda Christ[1], Sebastian Kapell[2], Georgios Mermelekas[3], Björn Evertsson[4], Helena Sork[5], Safa Bazaz[6], Oskar Gustafsson[6], Michal J. Sobkowiak[1], Eduardo I. Cardenas[7], Viviana Villa[8], Roberta Ricciarelli[8,9], Johan K. Sandberg[1], Jonas Bergquist[10], Andrea Sturchio[11,12], Per Svenningsson[11], Tarja Malm[13], Alberto J. Espay[12], Maria Pernemalm[3], Anders Lindén[7,14], Jonas Klingström[1], Samir El Andaloussi[6] and Kariem Ezzat[6*]

[1]Center for Infectious Medicine, Department of Medicine Huddinge, Karolinska Institutet, Stockholm, Sweden.

[2]National Bioinformatics Infrastructure Sweden (NBIS), Science for Life Laboratory, Department of Biochemistry and Biophysics, Stockholm University, Stockholm, Sweden.

[3]Cancer Proteomics Mass Spectrometry, SciLifeLab, Department of Oncology and Pathology, Karolinska Institutet, Stockholm, Sweden.

[4]Department of Clinical Neuroscience and Centrum for Molecular Medicine, Karolinska Institutet, Stockholm, Sweden.

[5]Institute of Technology, University of Tartu, Tartu, Estonia.

[6]Department of Laboratory Medicine, Biomolecular and Cellular Medicine, Karolinska Institutet, Stockholm, Sweden.

[7]Division of Lung and Airway Research, Institute of Environmental Medicine, Karolinska Institutet, Stockholm, Sweden.

[8]Department of Experimental Medicine, Section of General Pathology, School of Medical and Pharmaceutical Sciences, University of Genoa, Genoa, Italy.

[9]IRCCS Ospedale Policlinico San Martino, Genoa, Italy.

[10]Department of Chemistry-Biomedical Center, Analytical Chemistry and Neuro Chemistry, Uppsala University, Uppsala, Sweden.

[11]Department of Clinical Neuroscience, Neuro Svenningsson, Karolinska Institutet, Stockholm, Sweden.

[12]James J. and Joan A. Gardner Family Center for Parkinson's disease and Movement Disorders, Department of Neurology, University of Cincinnati, Cincinnati, Ohio, USA.

[13]A.I. Virtanen Institute for Molecular Sciences, University of Eastern Finland, Kuopio, Finland.

[14]Karolinska Severe COPD Center, Department of Respiratory Medicine and Allergy, Karolinska University Hospital, Stockholm, Sweden.

*Correspondence should be addressed to: kariem.ezzat.ahmed@ki.se

Abstract

The corona virus (SARS-CoV-2) pandemic and the resulting long-term neurological complications in patients, known as long COVID, have renewed the interest in the correlation between viral infections and neurodegenerative brain disorders. While many viruses can reach the central nervous system (CNS) causing acute or chronic infections (such as herpes simplex virus 1, HSV-1), the lack of a clear mechanistic link between viruses and protein aggregation into amyloids, a characteristic of several neurodegenerative diseases, has rendered such a connection elusive. Recently, we showed that viruses can induce aggregation of purified amyloidogenic proteins via the direct physicochemical mechanism of heterogenous nucleation (HEN). In the current study, we show that the incubation of HSV-1 and SARS-CoV-2 with human cerebrospinal fluid (CSF) leads to the amyloid aggregation of several proteins known to be involved in neurodegenerative diseases, such as: APLP1 (amyloid beta precursor like protein 1), ApoE, clusterin, α2-macroglobulin, PGK-1 (phosphoglycerate kinase 1), ceruloplasmin, nucleolin, 14-3-3, transthyretin and vitronectin. Importantly, UV-inactivation of SARS-CoV-2 does not affect its ability to induce amyloid aggregation, as amyloid formation is dependent on viral surface catalysis via HEN and not its ability to replicate. Our results show that viruses can physically induce amyloid aggregation of proteins in human CSF, and thus providing a potential mechanism that may account for the association between persistent and latent/reactivating brain infections and neurodegenerative diseases.

Introduction

The COVID-19 pandemic is estimated to have caused more than 6 million deaths worldwide in addition to tremendous economic and societal disruptions. While lock-down measures and vaccines helped ameliorate the acute impact of the pandemic, millions of people continue to suffer from post-acute COVID syndrome, or what is commonly known as long COVID (1). Many of the symptoms associated with long COVID are neurological in nature, such as fatigue, frequent headaches, and so-called “brain fog”, which includes difficulties with memory and concentration (2–4). The large and increasing number of people with post-COVID neurological symptoms has renewed the interest in the link between viruses and neurodegenerative brain disorders. There have been similar findings with other post-viral syndromes, including herpes simplex virus 1 (HSV-1) and its link to Alzheimer’s disease (AD) (5) and likewise for influenza virus and Parkinson’s disease (PD) (6). More recently, a strong link has been found between Epstein-Barr virus and multiple sclerosis (7). However, several factors have complicated the understanding of the connection between viruses and neurodegeneration, including:

1. The prevalence of viral infection is usually much higher than the prevalence of neurodegenerative diseases. For example, while nearly two-thirds of the human population have been infected with HSV-1 (8), the prevalence of AD is less than 2% (9).

2. The latent or persistent nature of viral brain infections, which usually involves alternating cycles of latency and activation, together with the long course of neurodegenerative diseases make it difficult to establish accurate temporal causal links.
3. The lack of a mechanism linking viral infections to amyloid aggregates, a hallmark of neurodegenerative disease.

The first two factors relate to the nature of viral infections of the brain and its immune responses to viruses. Since excessive inflammation can lead to irreparable neuronal damage, the brain evolved as an "immune-privileged" organ, where immune responses are tightly balanced and limited in magnitude and duration to prevent tissue damage (10, 11). Thus, while viral access to the brain is generally restricted by physical barriers (skull and meninges) and physiological barriers (the blood-brain-barrier), the viruses that manage to reach the brain benefit from the immune privilege and establish long-term latent (non-replicating) or persistent (low-level replication) infections, which can be reactivated depending on the genetic background and the immune status of the host (12). Furthermore, the non-replicating or low-level-replication of latent or persistent infections makes it very difficult to accurately quantify viral presence in the brain. However, the differential reactivation patterns across individuals may explain the prevalence gap between viral infections and neurodegenerative diseases, where some people are more susceptible than others to the long-term effects of chronic infections. Additionally, more sensitive detection methods are helping to better spatially and temporally correlate viruses with particular neurodegenerative pathologies. For example, RNAscope, a highly sensitive in-situ RNA hybridization method, has recently been utilized to differentiate between latent and lytic transcripts in human brain tissue and in the brains of AD mouse models infected with HSV-1, a result that was not attainable by normal qPCR (13). The same technique was used to show that SARS-CoV-2 infects cortical neurons in the brains of a subgroup of COVID-19 patients and induces AD-like neuropathology, including amyloid aggregation (14). Additionally, the proximity of the appearance of neurological symptoms to SARS-CoV-2 infection and the availability of large datasets from patients are enabling better causal correlations to be made. This has been demonstrated recently in a study of UK biobank participants, which identified significant longitudinal effects of SARS-CoV-2 infection on the brains of infected individuals, such as a reduction in grey matter thickness and global brain volume, compared to controls (15).

The third factor that put into question viral involvement in neurodegenerative diseases was the early finding that brain material inactivated by exposure to ultraviolet (UV) light can induce amyloid aggregation and neurodegeneration when inoculated into naive brains (16, 17). Since UV light inactivates nucleic acids, the agent inducing amyloid protein aggregation was hypothesized to be non-viral in nature, protein-only (prion), since viruses require nucleic acids for propagation (18). Protein-only prions are hypothesized to carry the conformational information required to template the transformation of normal proteins into amyloids (19). However, we have demonstrated earlier that viruses, including HSV-1 and respiratory syncytial virus (RSV), can induce amyloid

aggregation of amyloidogenic proteins via the physicochemical mechanism of heterogenous nucleation (HEN) in the absence of a protein seed acting as a conformational template (20). Recently, we outlined a theoretical framework that governs this process, illustrating that amyloid formation is a spontaneous folding event that is thermodynamically favorable under the conditions of supersaturation and nucleation and not a templated replication process (21). We have also recently demonstrated that, due to the highly stable and inert nature of amyloids, toxicity in amyloid pathologies might be more dependent on protein sequestration in the insoluble amyloid form (loss-of-function toxicity) rather than direct toxicity from the aggregates (gain-of-function toxicity) (21–23).

In the current study, we show that HSV-1 and UV-inactivated SARS-CoV-2 induce amyloid aggregation of proteins in human cerebrospinal fluid (CSF) ex-vivo. Using mass spectrometry-based proteomics to analyze the virus-induced amyloids, we identify several proteins that have been previously found in plaques from patients with neurodegenerative diseases. Our results indicate that viruses are mechanistically capable of directly triggering amyloid aggregation of proteins in human CSF.

Results

HSV-1 and SARS-CoV-2 induce protein aggregation in the CSF

To determine whether viral particles can catalyze amyloid aggregation of proteins in a complex human biofluid at their native concentration, we incubated live HSV-1 virus and UV-inactivated SARS-CoV-2 virus with CSF harvested from healthy individuals. We traced the ability of the viruses to induce amyloid formation using the thioflavin-T (ThT)-assay, where ThT fluorescence is enhanced upon binding to amyloid fibrils (24). Both viruses were able to induce amyloid aggregation of proteins in the CSF, while CSF with no virus added did not display any substantial signal for increasing amyloid aggregation over time (Figure 1. A and B). Additional controls, including non-infected cell medium and virus-only, produced a much lower signal, which is similar to what we reported earlier with purified amyloidogenic proteins (20). The maximum ThT fluorescence enhancement obtained from the viral treated CSF was significantly higher than all the controls (Supplementary Figure 1.). In addition, we used transmission electron microscopy (TEM) to visualize amyloid formation induced by the viruses in the CSF. We found multiple fibrillar amyloid structures interacting at the surface of HSV-1 (Figure 1. C & D) and SARS-CoV-2 (Figure 1. E & F), suggestive of surface-mediated catalytic nucleation (HEN) events.

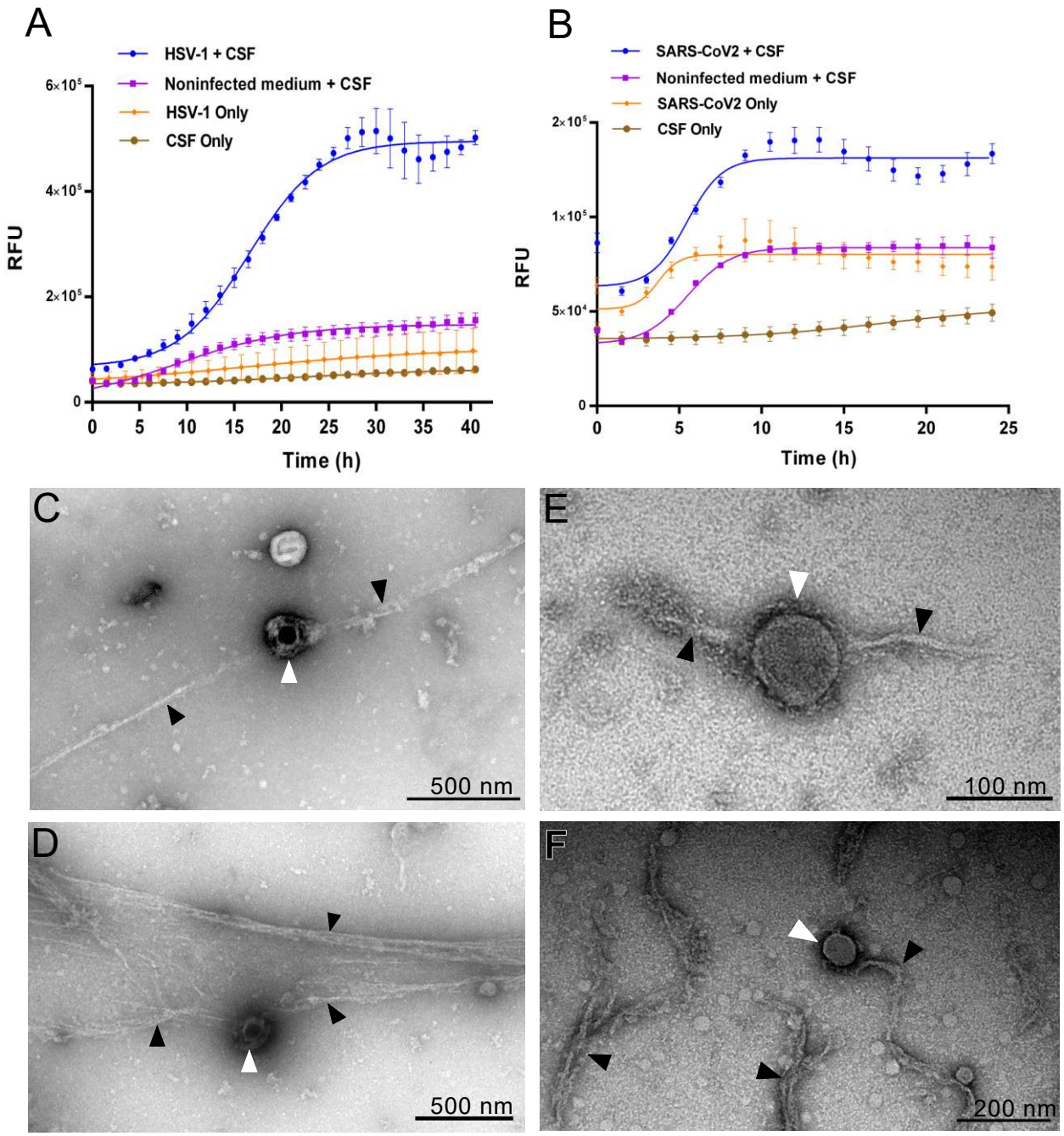

Figure 1. HSV-1 and SARS-CoV-2 induce amyloid aggregation of proteins in human CSF. CSF was incubated with HSV-1(**A**) or UV-inactivated-SARS-CoV-2 (**B**) and ThT solution. Fluorescence was measured at 440 nm excitation and 480 nm emission over 48 h at 37 °C. Means ± SEM of 8 replicates with CSF from two different individuals are shown. RFU = relative fluorescent unit. Negatively stained TEM images of HSV-1 (**C, D**) or UV-inactivated-SARS-CoV-2 (**E, F**) HSV-1 incubated with CSF for 48 h at 37 °C. White arrows indicate viral particles and black arrows indicate amyloid fibrillar structures.

Proteomic analysis of the viral-induced amyloid aggregates

To characterize the proteins present in the amyloid fractions, we collected and purified the amyloid aggregates induced by the viruses. We applied a protocol that involved using 4% SDS to remove the associated non-amyloid proteins, followed by washing, centrifugation, then solubilization of the amyloid fraction in 99% formic acid, which is among the few reagents that can solubilize the highly stable amyloid structures (25). In the proteomic analysis, we found that a large set of proteins was enriched in the virus-induced amyloid fractions compared to those present in untreated CSF (Figure 2. & Supplementary Table 1.). In total, 279 proteins were enriched in the virus-induced amyloid fractions compared to untreated CSF. More than 40% (n= 113) of the enriched proteins were shared in the amyloid fractions induced by both viruses, while about 37% (n= 102) were unique for the HSV-1-induced amyloid fraction, and 23% (n= 64) unique for the SARS-CoV-2-induced amyloid fraction. The large overlap between the sets of proteins enriched by the two viruses indicates that certain proteins in the CSF are more vulnerable to aggregation catalysts, most likely due to their high expression close to their supersaturation levels (26, 27). Previous proteomic studies have shown that a multitude of proteins can be found in amyloid plaques harvested from patients (28, 29). We found 135 proteins (Supplementary table 2) previously reported in plaques harvested from AD patients (28), including established components such as APLP1 (amyloid beta precursor like protein 1), ApoE, clusterin and α2-macroglobulin. Moreover, we identified proteins that have been linked to PD (30) such as ceruloplasmin, nucleolin, 14-3-3 and PGK-1 (phosphoglycerate kinase 1), and proteins related to other amyloid pathologies including transthyretin (TTR) and vitronectin (31). These results demonstrate that viral particles can efficiently catalyze the amyloid aggregation of a plethora of proteins in human CSF.

Discussion

While viruses have long been implicated in neurodegenerative diseases, it has been difficult to establish a mechanistic link. However, the large number of patients developing post-COVID neurological symptoms and the extensive data available from studying COVID-19 patients are starting to shed light on the possible causative role of viruses in chronic neurological disorders. A recent longitudinal study of 785 UK biobank participants demonstrated that SARS-CoV-2 infection led to a significant reduction in grey matter thickness and global brain volume, in addition to greater cognitive decline in infected individuals compared to non-infected controls (15). These longitudinal results corroborated previous observations about the detrimental effects of SARS-CoV-2 infection on the brain and cognition of infected individuals (4, 32). Furthermore, in older adults (age ≥65 years), COVID-19 patients were shown to have significantly higher risk for a new diagnosis of AD within 360 days after the initial COVID-19 diagnosis, in comparison with age-matched controls (33). Moreover, results from recent studies in animal models and in brain tissue of COVID19- patients suggest that SARS-CoV-2 infection of the brain is associated with amyloid protein aggregation (14, 34). In addition, several SARS-CoV-2 proteins have been shown

to have amyloidogenic potential (35, 36). Similar findings have been previously demonstrated for HSV-1, where HSV-1 reactivation was shown to increase AD risk (37), and HSV-1 infection was shown to induce amyloid aggregation in animal models (20, 38, 39). Thus, in parallel with the advancements in etiologically connecting viruses to neurodegenerative diseases, it is also important to uncover the pathophysiological mechanisms linking the two.

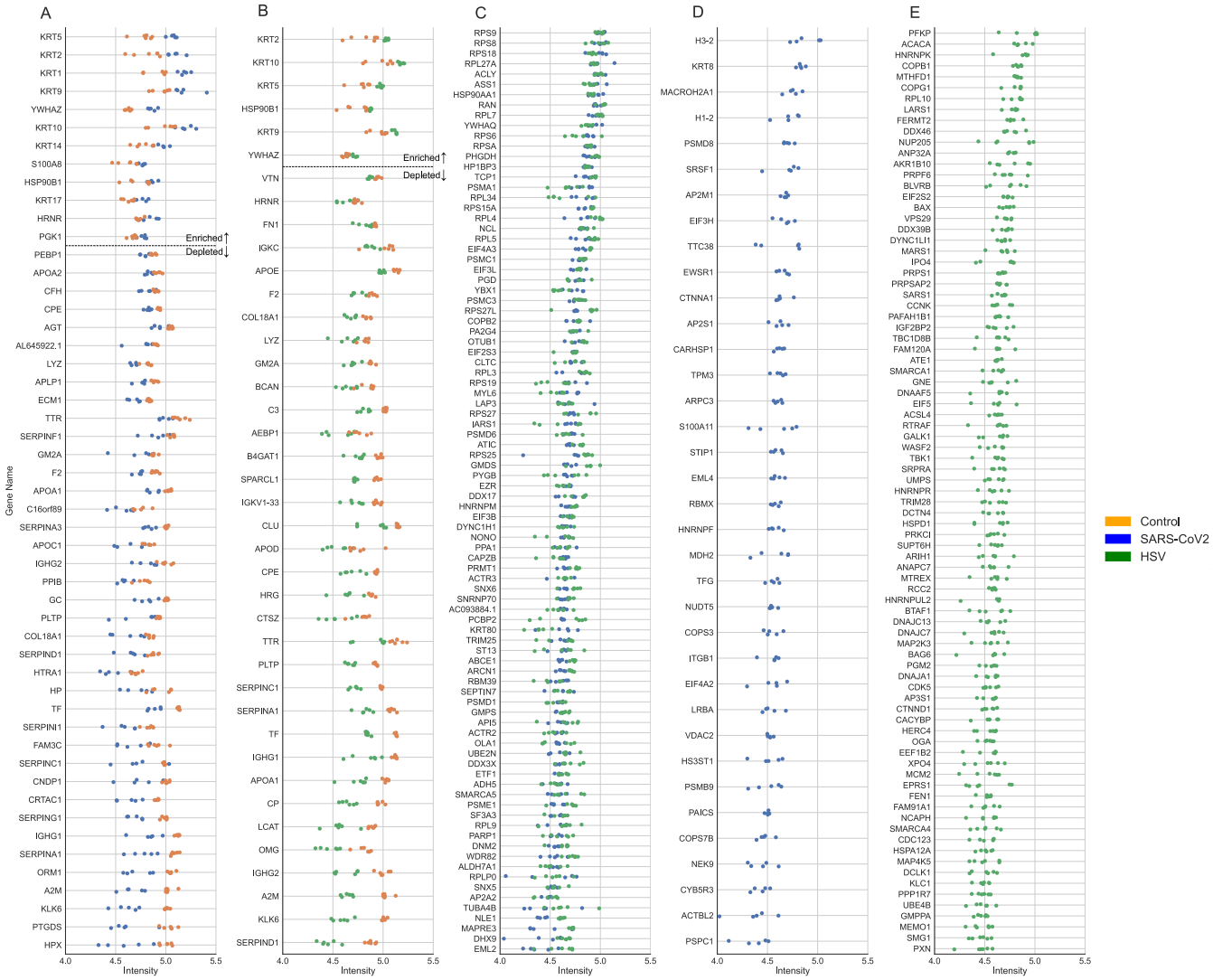

Figure 2. Proteins enriched in viral-induced amyloid fractions. (A-B) Differentially expressed proteins detected in both SARS-CoV-2-induced or HSV-1-induced amyloid fractions compared to control untreated CSF, assessed using a linear model (limma). All listed proteins had an adjusted p-value < 0.05 (Benjamini-Hochberg correction). C) Proteins detected in both SARS-CoV-2-induced and HSV-1-induced amyloid fractions but never in untreated CSF control samples. (D-E) Proteins uniquely detected in either SARS-CoV-2-induced or HSV-1-induced amyloid fractions but never in CSF control samples. (A-E) For all values local regression normalization (cyclic loess) were performed on protein intensity followed by Log2 transformation. 6 replicates with CSF from two different individuals were analyzed.

We have previously shown that viruses can directly induce amyloid aggregation of well-known amyloidogenic proteins such as amyloid-β peptide 1-42 (Aβ42) and amylin via HEN by acting as catalytic surfaces for nucleation (20). In a recent review, we outlined the physicochemical and thermodynamic basis of this interaction in light of the classical nucleation theory, where the presence of viral surfaces lowers the energy barrier for the phase transition of proteins from the soluble form into the solid amyloid form (21). This phase transition is spontaneous under conditions of supersaturation after crossing the nucleation barrier. Moreover, any protein sequence possesses the information necessary to adopt the amyloid conformation (cross-β), with no requirement for a protein seed/prion to act as a conformational template. In the current study, we show that HSV-1 and UV-inactivated SARS-CoV-2 catalyze amyloid aggregation of a multitude of proteins in their native environment and at their physiologic concentration in human CSF. This result further supports the notion that protein aggregation is a function of the recipient environment in terms of the concentration of specific proteins that is close to their limit of solubility (supersaturation) and their ability to interact with nucleating surfaces (26, 27, 40). Supersaturation provides the molecular proximity required to favor the generic *inter*molecular interactions necessary for amyloid formation over the specific *intra*molecular interactions required for native folding, with surfaces acting as nucleation sites that catalyze phase transition by lowering the interfacial energy barrier (21). In this physical sense, UV-inactivation should not, and did not, prevent SARS-CoV-2 viral particles from catalyzing amyloid nucleation on their surfaces. Indeed, in our current study, both live HSV-1 and UV-inactivated SARS-CoV-2 induced amyloid aggregation of a highly overlapping set of proteins. Thus, the resistance of infectious amyloidogenic agents to UV inactivation, which was demonstrated early on (16, 17) and was taken as evidence of the non-viral nature of such agents (18, 19), should be reconsidered. UV-inactivation, while it deactivates viral nucleic acids, does not affect the ability of viruses or other membranous structures to act as catalytic surfaces that induce amyloid aggregation. Importantly, the ability of viruses to invade the CNS and replicate, together with their ability to catalyze amyloid nucleation via HEN, make them more likely causes of amyloid aggregation in the brain compared to seed/prion transmission, which has been demonstrated only via the artificial procedure of direct injection into the brain.

Furthermore, we applied mass spectrometry-based proteomics to identify the proteins that were enriched in the amyloid fraction triggered by the two viruses compared to the normal CSF proteome. We found several proteins that were induced to form amyloids by HSV-1 and SARS-CoV-2, many of which are known to be involved in neurodegenerative diseases and have been reported before to be present in amyloid plaques harvested from patients. For example, APLP1, which is highly homologous to APP (amyloid precursor protein), is present in the plaques in the subiculum and entorhinal cortex in AD (41, 42). ApoE is very commonly found in amyloid plaques, not only in AD, but also in kuru and Creutzfeldt-Jakob disease (43, 44). Furthermore, ApoE is one of the major genetic risk factors for AD and has been shown to interact with Aβ in a variety of ways (45). The same has been demonstrated for clusterin and α2-macroglobulin, which were shown to be associated with amyloid plaques in AD (46, 47). We

also identified other proteins that are often related to PD. For example, PGK1, whose deficiency is associated with young-onset parkinsonism (48), and ceruloplasmin and nucleolin, which have been shown to be lower in patients with PD compared to controls (30, 49). Interestingly, 14-3-3 proteins, were also identified in the viral induced amyloid fractions. The 14-3-3 protein family is highly abundant in the brain and has been found to accumulate within Lewy bodies in PD and in plaques and tangles in AD (50–54). They have also been shown to interact with SARS-CoV-2 (55). Moreover, we identified proteins commonly associated with systemic amyloidosis such as transthyretin (TTR) and vitronectin (31, 56). However, both have also been detected in CNS amyloids (57, 58). Other proteins identified in the viral-induced amyloid fractions include immunological components (e.g. IGHG1, IGHG2, complement C3), ribosomal proteins (e.g. ribosomal protein L27a, ribosomal protein L3, ribosomal protein L34), extracellular matrix proteins (e.g. collagen type XVIII alpha 1 chain, keratin 9, fibronectin 1) cytoskeleton proteins (e.g. actin-related protein 2, microtubule-associated protein RP/EB family member 3), heatshock proteins (e.g. HSP 60, 70 and 90) and proteasome proteins (e.g. proteasome 26S subunit alpha 1, proteasome activator subunit 1). While many of these proteins have been detected before in patient-derived plaques (28), further studies are required to address their contribution to a particular disease. However, many of the amyloid-enriched proteins possess important functions in the brain, which suggests that catalyzing protein aggregation and subsequent depletion and loss-of-function might be one mechanism by which viruses cause neurodegeneration. We have recently demonstrated that protein depletion and related loss-of-function is more pathologically important than plaque burden in AD, where high levels of soluble Aβ42 in the CSF were associated with preserved cognition even in individuals with high amyloid plaque burden (22). Depletion of soluble Aβ42 in the CSF, which is a recognized feature of many neurodegenerative disorders, has been demonstrated in patients with post-COVID neurological symptoms (59), suggesting that protein depletion post-infection might contribute to the neurological symptoms. Further studies examining the levels of more CSF proteins in post-COVID patients compared to controls could reveal additional information on this potential pathophysiological mechanism.

In conclusion, we have demonstrated that HSV-1 and SARS-CoV-2 induce aggregation of a multitude of proteins in human CSF. We have also demonstrated that UV-inactivation does not destroy the ability of viral particles to act as a catalytic surface for amyloid nucleation. Hence, the role of viruses as causative agents of protein aggregation in neurodegeneration needs to be reevaluated in light of the important catalytic role they can play in this process. Understanding the mechanisms by which viruses may cause neurological disorders is especially important due to the SARS-CoV-2 pandemic which has led to a large number of people suffering from long-COVID neurological symptoms post infection. The availability of large and accurate databases of patients together with more sensitive methods to detect viruses in the brain are making the link between virus infection and neurodegenerative brain disorders more robust. Taken together with other mechanisms that might lead to viral-induced brain damage

(inflammation, autoimmunity, blood-clots) (60), viral-induced protein aggregation via HEN can contribute to neuronal pathology by catalyzing the aggregation and precipitation of important neuronal proteins.

Materials and methods

Viral production

For HSV-1, strain F HSV-1 stocks were prepared by infecting African green monkey kidney (vero) cells at 80–90% confluency in serum-free VP-SFM (Gibco). The virus was harvested 2 d after infection. Cells were subjected to two freeze-thaw cycles and spun at 20,000 g for 10 min to remove cell debris. Clarified supernatant was aliquoted and stored at -80°C until use. Non-infected cell medium was prepared with the same procedure without viral infection. Plaque assay was used to determine viral titers. 10-fold dilutions of virus were added onto vero cells for 1 h at 37°C, then inoculum was removed, and fresh medium containing 0.5% carboxymethyl cellulose (Sigma Aldrich) was added. Cells were fixed and stained 2d later with a 0.1% crystal violet solution and the number of plaques was counted. For SARS-CoV-2 stock production, Vero E6 cells were infected with the SARS-CoV-2 wild type (isolate SARS-CoV-2/human/SWE/01/2020; Genbank accession: MT093571) in VP-SFM (Gibco). The virus was harvested at day three, four and five post-infection and centrifuged at 1000 g for 6 min to remove cells debris. The clarified supernatant was further centrifuged at 45000 g for 4h. After centrifugation, the supernatant was removed, and the virus pellet was resuspended in fresh VP-SFM. Viral titers were determined via end-point-dilution assay. For UV-inactivation, the virus stock was incubated under UV-light for 3 x 1.5 min, and complete inactivation was confirmed by treating Vero E6 with the inactivated stock and observing no cytopathic effects (CPE) 5 days post-treatment.

CSF ethical permit and harvesting

CSF samples were collected at Karolinska University Hospital Huddinge. The collection and test were approved by the Regional Ethical Review Board in Stockholm (Diary number: 2020-03471 and 2009/2107-31-2). All CSF samples were pre-cleared by 400 × g for 10 min and subsequent 2,000 × g centrifugation for 10 min. After that aliquoted to a minimal volume of 500 µl and then frozen to -80°C, within 2 hours from sampling.

CSF amyloid aggregation

ThT (Sigma Aldrich) was prepared at 4 mM in MQ water. For the assay with HSV-1, 50µl of CSF were incubated with 150µl of 4 mM ThT solution and 100 µl of HSV-1 (2 x 10^7 PFU/ml), or non-infected supernatant. For the assay with UV-inactivated SARS-CoV-2, 25µl of CSF were incubated with 150µl of 4 mM ThT solution and 25µl of UV-inactivated SARS-CoV-2 (4.6 x 10^7 PFU/ml), or non-infected supernatant. UV-inactivated SARS-CoV-2 was

used instead of live SARS-CoV-2 for biosafety reasons since live SARS-CoV-2 was not safe to incubate in the spectrophotometer outside the BSL-3 laboratory. Controls included CSF only without virus and virus only without CSF, in both cases the missing volume was substituted with MQ water. ThT fluorescence was measured at 440 nm excitation and 480 nm emission in a black clear-bottom 96-well plates (Corning, USA) at 440 nm excitation and 480 nm emission at 10-15 min. intervals (from bottom with periodic shaking) over 24-48 h on SpectraMax i3 microplate reader (Molecular Devices, USA). Curves were fitted using GraphPad Prism software.

Electron Microscopy

For TEM, equal volumes (50 µl) of viruses (HSV-1 (2 x 10^7 PFU/ml) or UV-inactivated SARS-CoV-2 (4.6 x 10^7 PFU/ml) and CSF were incubated at 37 ˚C for 48 h. Samples were then applied to Formvar/carbon coated 200 mesh nickel grids (Agar Scientific, UK), then negatively stained using an aqueous solution of uranyl acetate (1%) and visualized.

Amyloid purification

Equal volumes (100 µl) of virus (HSV-1 (2 x 10^7 PFU/ml) or UV-inactivated SARS-CoV-2 (4.6 x 10^7 PFU/ml) and CSF were incubated at 37 ˚C for 48 h. Amyloid aggregates were then collected by spinning at 20 000 g for 15 min. at room temperature. The pellet was then washed 2x by vortexing in 100 µl lysis buffer (4% SDS, 25 mM HEPES pH 7.6, 1 mM DTT) for 2 min. followed by 15 min, 20 000 g centrifugation at room temperature. The pellet was then dissolved in 99% formic acid by vortexing for 2 min and sonication for 5 minutes. Formic acid was then removed by speedvacing at room temperature for 30 min. and the proteins were resuspended in 50 µl PBS for proteomic analysis.

Sample preparation for proteomics

The samples collected were lysed by 4 % SDS lysis buffer and prepared for mass spectrometry analysis using a modified version of the SP3 protein clean up and digestion protocol. In brief, all the amount of sample was alkylated with 4 mM Chloroacetamide. Sera-Mag SP3 bead mix (20 µl) was transferred into the protein sample together with 100% Acetonitrile to a final concentration of 70 %. The mix was incubated under rotation at room temperature for 18 min. The mix was placed on the magnetic rack and the supernatant was discarded, followed by two washes with 70 % ethanol and one with 100 % acetonitrile. The beads-protein mixture was reconstituted in 100 µl LysC buffer (0.5 M Urea, 50 mM HEPES pH: 7.6 and 1:50 enzyme (LysC) to protein ratio) and incubated overnight. Finally, trypsin was added in 1:50 enzyme to protein ratio in 100 µl 50 mM HEPES pH 7.6 and incubated overnight followed by SP3 peptide clean up. The peptide mix was suspended in 15 µl LC mobile phase A and 5 µl was injected on the LC-MS/MS system.

Mass spectrometry

LC-ESI-MS/MS, Q-Exactive Online LC-MS was performed using a Dionex UltiMate™ 3000 RSLCnano System coupled to a Q-Exactive mass spectrometer (Thermo Scientific). 5 uL was injected from each sample. Samples were trapped on a C18 guard desalting column (Acclaim PepMap 100, 75µm x 2 cm, nanoViper, C18, 5 µm, 100 Å), and separated on a 50 cm long C18 column (Easy spray PepMap RSLC, C18, 2 µm, 100Å, 75 µmx15cm). The nano capillary solvent A was 95% water, 5%DMSO, 0.1% formic acid; and solvent B was 5% water, 5% DMSO, 95% acetonitrile, 0.1% formic acid. At a constant flow of 0.25 µl min^{-1}, the curved gradient went from 6%B up to 43%B in 180 min, followed by a steep increase to 100%B in 5 min. FTMS master scans with 60,000 resolution (and mass range 300-1500 m/z) were followed by data-dependent MS/MS (30 000 resolution) on the top 5 ions using higher energy collision dissociation (HCD) at 30% normalized collision energy. Precursors were isolated with a 2m/z window. Automatic gain control (AGC) targets were 1e6 for MS1 and 1e5 for MS2. Maximum injection times were 100ms for MS1 and MS2. The entire duty cycle lasted ~2.5s. Dynamic exclusion was used with 60s duration. Precursors with unassigned charge state or charge state 1 were excluded. An underfill ratio of 1% was used.

Bioinformatics

Orbitrap raw MS/MS files were converted to mzML format using msConvert from the ProteoWizard tool suite (61) and processed with a pipeline built using Nextflow (62) with MSGF+ (63) as a peptide identification search engine, Percolator for target-decoy scoring (64) and Hardklor/Kronik (65) for quantifying MS1 peptide features. MSGF+ settings included precursor mass tolerance of 10 ppm, fully-tryptic peptides, maximum peptide length of 50 amino acids and a maximum charge of 6. Fixed modification was carbamidomethylation on cysteine residues, a variable modification was used for oxidation on methionine residues. PSMs found at 1% FDR (false discovery rate) were used to infer protein identities. All searches were done against the human protein subset of Ensembl 102 and custom-built peptide database. 6 replicates with CSF from two different individuals were analyzed. Output from pipeline was filtered, removing protein identifications present in less that 4/6 replicates per sample group any missing values after filtering was imputed using the MissForest method (66). Protein intensity values were then normalized using the cyclic-loess method with the NormalizerDE package (67), differentially expression analysis conducted using LIMMA (68).

Acknowledgements

Support by NBIS (National Bioinformatics Infrastructure Sweden) is gratefully acknowledged.

References

1. Misra,S., Kolappa,K., Prasad,M., Radhakrishnan,D., Thakur,K.T., Solomon,T., Michael,B.D., Winkler,A.S., Beghi,E., Guekht,A., *et al.* (2021) Frequency of neurologic manifestations in COVID-19. *Neurology*, **97**, E2269–E2281.

2. Mehandru,S. and Merad,M. (2022) Pathological sequelae of long-haul COVID. *Nat Immunol*, **23**, 194–202.

3. Serena Spudich,A.N. (2022) Nervous system consequences of COVID-19: Neurological symptoms highlight the need to understand pathophysiologic mechanisms. *Science (1979)*, **375**, 2020–2023.

4. Hampshire,A., Chat,A., Mphil,M., Jolly,A., Trender,W., Hellyer,P.J., Giovane,M. del, Newcombe,V.F.J., Outtrim,J.G., Warne,B., *et al.* (2022) Multivariate profile and acute-phase correlates of cognitive deficits in a COVID-19 hospitalised cohort. **47**, 1–10.

5. Itzhaki,R.F., Lathe,R., Balin,B.J., Ball,M.J., Bearer,E.L., Braak,H., Bullido,M.J., Carter,C., Clerici,M., Cosby,S.L., *et al.* (2016) Microbes and Alzheimer's disease. *Journal of Alzheimer's Disease*, **51**, 979–984.

6. Dowd,E. and McKernan,D.P. (2021) Back to the future: lessons from past viral infections and the link with Parkinson's disease. *Neuronal Signal*, **5**, 1–8.

7. Bjornevik,K., Cortese,M., Healy,B.C., Kuhle,J., Mina,M.J., Leng,Y., Elledge,S.J., Niebuhr,D.W., Scher,A.I., Munger,K.L., *et al.* (2022) Longitudinal analysis reveals high prevalence of Epstein-Barr virus associated with multiple sclerosis. *Science (1979)*, **375**, 296–301.

8. James,C., Harfouche,M., Welton,N.J., Turner,K.M.E., Abu-Raddad,L.J., Gottlieb,S.L. and Looker,K.J. (2020) Herpes simplex virus: global infection prevalence and incidence estimates, 2016. *Bull World Health Organ*, **98**, 315.

9. 2022 Alzheimer's disease facts and figures (2022) *Alzheimer's & Dementia*, **18**, 700–789.

10. Paludan,S.R. and Mogensen,T.H. (2021) Constitutive and latent immune mechanisms exert 'silent' control of virus infections in the central nervous system. *Curr Opin Immunol*, **72**, 158–166.

11. Bergmann,C.C., Lane,T.E. and Stohlman,S.A. (2006) Coronavirus infection of the central nervous system: Host-virus stand-off. *Nat Rev Microbiol*, **4**, 121–132.

12. Forrester,J. v., McMenamin,P.G. and Dando,S.J. (2018) CNS infection and immune privilege. *Nat Rev Neurosci*, **19**, 655–671.

13. Zhang,S., Zeng,J., Zhou,Y., Gao,R., Rice,S., Guo,X., Liu,Y., Feng,P. and Zhao,Z. (2022) Simultaneous Detection of Herpes Simplex Virus Type 1 Latent and Lytic Transcripts in Brain Tissue. *ASN Neuro*, **14**, 1–13.

14. Shen,W.-B., Logue,J., Yang,P., Baracco,L., Elahi,M., Reece,E.A., Wang,B., Li,L., Blanchard,T.G., Han,Z., *et al.* (2022) SARS-CoV-2 invades cognitive centers of the brain and induces Alzheimer's-like neuropathology. *bioRxiv*, 10.1101/2022.01.31.478476.

15. Douaud,G., Lee,S., Alfaro-Almagro,F., Arthofer,C., Wang,C., McCarthy,P., Lange,F., Andersson,J.L.R., Griffanti,L., Duff,E., *et al.* (2022) SARS-CoV-2 is associated with changes in brain structure in UK Biobank. *Nature*, 10.1038/s41586-022-04569-5.

16. Alper,T., Cramp,W.A., Haig,D.A. and Clarke,M.C. (1967) Does the agent of scrapie replicate without nucleic acid? *Nature*, **214**, 764–766.

17. Alper,T. (1972) The nature of the scrapie agent. *J Clin Pathol*, **25**, 154–155.

18. Prusiner,S.B. (1982) Novel proteinaceous infectious particles cause scrapie. *Science (1979)*, **216**, 136–144.

19. Ayers,J.I., Paras,N.A. and Prusiner,S.B. (2020) Expanding spectrum of prion diseases. *Emerg Top Life Sci*, 10.1042/etls20200037.

20. Ezzat,K., Pernemalm,M., Pålsson,S., Roberts,T.C., Järver,P., Dondalska,A., Bestas,B., Sobkowiak,M.J., Levänen,B., Sköld,M., *et al.* (2019) The viral protein corona directs viral pathogenesis and amyloid aggregation. *Nature Communications 2019 10:1*, **10**, 1–16.

21. Ezzat,K., Sturchio,A. and Espay,A.J. (2022) Proteins Do Not Replicate, They Precipitate: Phase Transition and Loss of Function Toxicity in Amyloid Pathologies. *Biology (Basel)*, **11**, 535.

22. Sturchio,A., Dwivedi,A.K., Young,C.B., Malm,T., Marsili,L., Sharma,J.S., Mahajan,A., Hill,E.J., Andaloussi,S. el, Poston,K.L., *et al.* (2021) High cerebrospinal amyloid-β 42 is associated with normal cognition in individuals with brain amyloidosis. *EClinicalMedicine*, **000**, 100988.

23. Espay,A.J., Sturchio,A., Schneider,L.S. and Ezzat,K. (2021) Soluble Amyloid-β Consumption in Alzheimer's Disease. *Journal of Alzheimer's Disease*, 10.3233/jad-210415.

24. Biancalana,M. and Koide,S. (2010) Molecular mechanism of Thioflavin-T binding to amyloid fibrils. *Biochimica et Biophysica Acta (BBA) - Proteins and Proteomics*, **1804**, 1405–1412.

25. Mori,H., Takio,K., Ogawara,M. and Selkoe,D.J. (1992) Mass spectrometry of purified amyloid β protein in Alzheimer's disease. *Journal of Biological Chemistry*, **267**, 17082–17086.

26. Ciryam,P., Kundra,R., Morimoto,R.I., Dobson,C.M. and Vendruscolo,M. (2015) Supersaturation is a major driving force for protein aggregation in neurodegenerative diseases. *Trends Pharmacol Sci*, **36**, 72–77.

27. Freer,R., Sormanni,P., Ciryam,P., Rammner,B., Rizzoli,S.O., Dobson,C.M. and Vendruscolo,M. (2019) Supersaturated proteins are enriched at synapses and underlie cell and tissue vulnerability in Alzheimer's disease. *Heliyon*, **5**, e02589.

28. Drummond,E., Nayak,S., Faustin,A., Pires,G., Hickman,R.A., Askenazi,M., Cohen,M., Haldiman,T., Kim,C., Han,X., *et al.* (2017) Proteomic differences in amyloid plaques in rapidly progressive and sporadic Alzheimer's disease. *Acta Neuropathol*, **133**, 933–954.

29. Liao,L., Cheng,D., Wang,J., Duong,D.M., Losik,T.G., Gearing,M., Rees,H.D., Lah,J.J., Levey,A.I. and Peng,J. (2004) Proteomic characterization of postmortem amyloid plaques isolated by laser capture microdissection. *Journal of Biological Chemistry*, **279**, 37061–37068.

30. Dixit,A., Mehta,R. and Singh,A.K. (2019) Proteomics in Human Parkinson's Disease: Present Scenario and Future Directions. *Cell Mol Neurobiol*, **39**, 901–915.

31. Kourelis,T. v., Dasari,S.S., Dispenzieri,A., Maleszewski,J.J., Redfield,M.M., Fayyaz,A.U., Grogan,M., Ramirez-Alvarado,M., Abou Ezzeddine,O.F. and McPhail,E.D. (2020) A Proteomic Atlas of Cardiac Amyloid Plaques. *JACC CardioOncol*, **2**, 632–643.

32. Matschke,J., Lütgehetmann,M., Hagel,C., Sperhake,J.P., Schröder,A.S., Edler,C., Mushumba,H., Fitzek,A., Allweiss,L., Dandri,M., *et al.* (2020) Neuropathology of patients with COVID-19 in Germany: a post-mortem case series. *Lancet Neurol*, **4422**, 1–11.

33. Wang,L., Davis,P.B., Volkow,N.D., Berger,N.A., Kaelber,D.C. and Xu,R. (2022) Association of COVID-19 with New-Onset Alzheimer's Disease. *Journal of Alzheimer's Disease*, **Preprint**, 1–4.

34. Käufer,C., Schreiber,C.S., Hartke,A.-S., Denden,I., Stanelle-Bertram,S., Beck,S., Kouassi,N.M., Beythien,G., Becker,K., Schreiner,T., *et al.* (2022) Microgliosis and neuronal proteinopathy in brain persist beyond viral clearance in SARS-CoV-2 hamster model. *EBioMedicine*, **79**, 103999.

35. Nyström,S. and Hammarström,P. (2022) Amyloidogenesis of SARS-CoV-2 Spike Protein. *J Am Chem Soc*, 10.1021/jacs.2c03925.

36. Charnley,M., Islam,S., Bindra,G.K., Engwirda,J., Ratcliffe,J., Zhou,J., Mezzenga,R., Hulett,M.D., Han,K., Berryman,J.T., *et al.* (2022) Neurotoxic amyloidogenic peptides in the proteome of SARS-COV2: potential implications for neurological symptoms in COVID-19. *Nat Commun*, **13**, 3387.

37. Lövheim,H., Gilthorpe,J., Adolfsson,R., Nilsson,L.-G. and Elgh,F. (2014) Reactivated herpes simplex infection increases the risk of Alzheimer's disease. *Alzheimers Dement*, **11**, 1–7.

38. Wozniak,M.A., Itzhaki,R.F., Shipley,S.J. and Dobson,C.B. (2007) Herpes simplex virus infection causes cellular beta amyloid accumulation and secretase upregulation. *Neurosci Lett*, **429**, 95–100.

39. de Chiara,G., Piacentini,R., Fabiani,M., Mastrodonato,A., Marcocci,M.E., Limongi,D., Napoletani,G., Protto,V., Coluccio,P., Celestino,I., *et al.* (2019) Recurrent herpes simplex virus-1 infection induces hallmarks of neurodegeneration and cognitive deficits in mice. *PLoS Pathog*, **15**, e1007617.

40. Ciryam,P., Tartaglia,G.G., Morimoto,R.I., Dobson,C.M. and Vendruscolo,M. (2013) Widespread Aggregation and Neurodegenerative Diseases Are Associated with Supersaturated Proteins. *Cell Rep*, **5**, 781–790.

41. Bayer,T.A., Paliga,K., Weggen,S., Wiestier,O.D., Beyreuther,K. and Multhaup,G. (1997) Amyloid precursor-like protein 1 accumulates in neuritic plaques in Alzheimer's disease. *Acta Neuropathol*, **94**, 519–524.

42. McNamara,M.J., Ruff,C.T., Wasco,W., Tanzi,R.E., Thinakaran,G. and Hyman,B.T. (1998) Immunohistochemical and in situ analysis of amyloid precursor-like protein-1 and amyloid precursor-like protein-2 expression in Alzheimer disease and aged control brains. *Brain Res*, **804**, 45–51.

43. Wisniewski,T. and Frangione,B. (1992) Apolipoprotein E: A pathological chaperone protein in patients with cerebral and systemic amyloid. *Neurosci Lett*, **135**, 235–238.

44. Namba,Y., Tomonaga,M., Kawasaki,H., Otomo,E. and Ikeda,K. (1991) Apolipoprotein E immunoreactivity in cerebral amyloid deposits and neurofibrillary tangles in Alzheimer ' s disease and kuru plaque amyloid in Creutzfeldt-Jakob disease. **541**, 163–166.

45. Yu,J., Tan,L. and Hardy,J. (2014) Apolipoprotein E in Alzheimer ' s Disease : An Update. 10.1146/annurev-neuro-071013-014300.

46. Oh,S.-B., Kim,M.S., Park,S., Son,H., Kim,S.-Y., Kim,M.-S., Jo,D.-G., Tak,E. and Lee,J.-Y. (2018) Clusterin contributes to early stage of Alzheimer's disease pathogenesis. *Brain Pathology*, 10.1111/bpa.12660.

47. Kovacs,D.M. (2000) α2-Macroglobulin in late-onset Alzheimer's disease. *Exp Gerontol*, **35**, 473–479.

48. Morales-Briceño,H., Ha,A.D., London,K., Farlow,D., Chang,F.C.F. and Fung,V.S.C. (2019) Parkinsonism in PGK1 deficiency implicates the glycolytic pathway in nigrostriatal dysfunction. *Parkinsonism Relat Disord*, **64**, 319–323.

49. Caudle,W.M., Kitsou,E., Li,J., Bradner,J. and Zhang,J. (2009) A role for a novel protein, nucleolin, in Parkinson's disease. *Neurosci Lett*, **459**, 11–15.

50. Umahara,T., Uchihara,T., Tsuchiya,K., Nakamura,A., Iwamoto,T., Ikeda,K. and Takasaki,M. (2004) 14-3-3 proteins and zeta isoform containing neurofibrillary tangles in patients with Alzheimer's disease. *Acta Neuropathol*, **108**, 279–286.

51. Gu,Q., Cuevas,E., Raymick,J., Kanungo,J. and Sarkar,S. (2020) Downregulation of 14-3-3 Proteins in Alzheimer's Disease. *Mol Neurobiol*, **57**, 32–40.

52. Berg,D., Riess,O. and Bornemann,A. (2003) Specification of 14-3-3 proteins in Lewy bodies [1]. *Ann Neurol*, **54**, 135.

53. Kawamoto,Y., Akiguchi,I., Nakamura,S., Honjyo,Y., Shibasaki,H. and Budka,H. (2002) 14-3-3 Proteins in Lewy bodies in Parkinson disease and diffuse Lewy body disease brains. *J Neuropathol Exp Neurol*, **61**, 245–253.

54. McFerrin,M.B., Chi,X., Cutter,G. and Yacoubian,T.A. (2017) Dysregulation of 14-3-3 proteins in neurodegenerative diseases with Lewy body or Alzheimer pathology. *Ann Clin Transl Neurol*, **4**, 466–477.

55. Vavougios,G.D. (2020) SARS-CoV-2 dysregulation of PTBP1 and YWHAE / Z gene expression : A primer of neurodegeneration. *Med Hypotheses*, **144**, 110212.

56. Ruberg,F.L., Grogan,M., Hanna,M., Kelly,J.W. and Maurer,M.S. (2019) Transthyretin Amyloid Cardiomyopathy: JACC State-of-the-Art Review. *J Am Coll Cardiol*, **73**, 2872–2891.

57. Sousa,L., Coelho,T. and Taipa,R. (2021) CNS Involvement in Hereditary Transthyretin Amyloidosis. *Neurology*, **97**, 1111–1119.

58. Shin,T.M., Isas,J.M., Hsieh,C.L., Kayed,R., Glabe,C.G., Langen,R. and Chen,J. (2008) Formation of soluble amyloid oligomers and amyloid fibrils by the multifunctional protein vitronectin. *Mol Neurodegener*, **3**, 1–12.

59. Ziff,O.J., Ashton,N.J., Mehta,P.R., Brown,R., Athauda,D., Heaney,J., Heslegrave,A.J., Benedet,A.L., Blennow,K., Checkley,A.M., *et al.* (2022) Amyloid processing in COVID-19-associated neurological syndromes. *J Neurochem*, **161**, 146–157.

60. Couzin-Frankel,J. and Mastin,A. (2022) Clues to long COVID. *Science (1979)*, **376**, 1261–1265.

61. Holman,J.D., Tabb,D.L. and Mallick,P. (2014) Employing ProteoWizard to convert raw mass spectrometry data. *Curr Protoc Bioinformatics*, 10.1002/0471250953.bi1324s46.

62. di Tommaso,P., Chatzou,M., Floden,E.W., Barja,P.P., Palumbo,E. and Notredame,C. (2017) Nextflow enables reproducible computational workflows. *Nat Biotechnol*, **35**, 316–319.

63. Kim,S. and Pevzner,P.A. (2014) MS-GF+ makes progress towards a universal database search tool for proteomics. *Nat Commun*, **5**.

64. The,M., MacCoss,M.J., Noble,W.S. and Käll,L. (2016) Fast and Accurate Protein False Discovery Rates on Large-Scale Proteomics Data Sets with Percolator 3.0. *J Am Soc Mass Spectrom*, **27**, 1719–1727.

65. Hoopmann,M.R., MacCoss,M.J. and Moritz,R.L. (2012) Identification of peptide features in precursor spectra using hardklör and krönik. *Curr Protoc Bioinformatics*, 10.1002/0471250953.bi1318s37.

66. Stekhoven,D.J. and Bühlmann,P. (2012) Missforest-Non-parametric missing value imputation for mixed-type data. *Bioinformatics*, **28**, 112–118.

67. Willforss,J., Chawade,A. and Levander,F. (2019) NormalyzerDE: Online Tool for Improved Normalization of Omics Expression Data and High-Sensitivity Differential Expression Analysis. *J Proteome Res*, **18**, 732–740.

68. Ritchie,M.E., Phipson,B., Wu,D., Hu,Y., Law,C.W., Shi,W. and Smyth,G.K. (2015) Limma powers differential expression analyses for RNA-sequencing and microarray studies. *Nucleic Acids Res*, **43**, e47.